

# Chapter 13

## Thermal Characterization of Graphitized Carbon Nanotube-Reinforced Ti64 Nanocomposites Synthesized by Field-Assisted Sintering Technique for Fuselage and Wing Box Applications



Adewale Oladapo Adegbenjo, Mary Ajimegoh Awotunde, Tien-Chien Jen, and Johan Herman Potgieter

### 1 Introduction

Despite their high demand and attractiveness in high-performance, lightweight, and competitive, high-strength applications, titanium (Ti) and its alloys have witnessed immense setback in usage as thermal materials owing to their unimpressive thermal characteristics at room and elevated temperatures (Adegbenjo et al., 2017a; Wang et al., 2015). For example, the thermal conductivity of Grade 1 Ti is typically lower than that anticipated normally for a metal, and alloys of Ti (Ti64 to be specific) most often display significantly lower or inferior thermal conductivities compared to that of the pure grade sample (Adegbenjo et al., 2019a; Işık & Kentli, 2014). Also, due to their low thermal conductivities and poor elastic modulus, the machining of Ti and its alloys becomes very difficult, thereby adversely impacting on tool life as the temperature at the tool and workpiece interface substantially increases while

---

A. O. Adegbenjo (✉)

Mechanical Engineering Department, Adeseun Ogundoyin Polytechnic, Eruwa, Nigeria

Department of Mechanical Engineering Science, University of Johannesburg, Johannesburg, South Africa

M. A. Awotunde

Centre for Nanoengineering and Tribocorrosion, University of Johannesburg, Johannesburg, Gauteng, South Africa

T.-C. Jen

Department of Mechanical Engineering Science, University of Johannesburg, Johannesburg, South Africa

J. H. Potgieter

School of Chemical and Metallurgical Engineering, University of The Witwatersrand, Johannesburg, South Africa

machining (Li et al., 2020a; Munir et al., 2018). Furthermore, the fields where Ti and its alloys are mostly employed, such as in the aerospace, defense, automotive, and nuclear industries, require that the materials are thermally stable, with high thermal conductivities (Babapoor et al., 2018).

In spite of the above mentioned pitfalls associated with the applications of Ti and its alloys, their demand keeps growing due to excellent compatibility with Carbon Fiber-Reinforced Plastic (CFRP) in respect to corrosion properties and coefficient of thermal expansion. For instance, it is reported that the amount of Ti employed in the low-fuel consumption aircrafts, where a large quantity of CFRP is used, accounts for more than twice the amount used in the conventional aircraft (Inagaki et al., 2014). However, a major problem with the applications of Ti and its alloys at high temperatures is embrittlement arising from oxygen contamination on the surface; hence, they are mostly used at operating temperatures between 500 and 600 °C. Consequently, Ti64 particularly is employed in the fabrication of wing boxes and the fuselage as it offers higher specific strength, competitive weight savings, and excellent fatigue strengths compared to nickel-based alloys. Nevertheless, Wang et al. (2015) opined that adiabatic shear failures are usually experienced in engineering applications where Ti products are required due to the relatively poor heat conduction characteristics of these materials. Hence, the need to enhance their thermal performances become crucial in order to make the best of this class of materials in these identified specialized areas of their applications.

Carbon nanotubes (CNTs) have been described by several researchers as a reliable reinforcing material for metal-based composites due to their superexcellent mechanical and thermal characteristics (Bhat et al., 2011; Chen et al., 2017; Kondoh et al., 2012; Lephuthing et al., 2020; Liu et al., 2020; Munir et al., 2017). MWCNTs display a thermal conductivity in excess of 3000 W/m K, which falls within the range of the quoted values for diamond crystal and in-plane graphite sheets (Munir et al., 2018). Thus, the addition of MWCNTs to Ti matrices is expected to positively affect the thermal characteristics of the resulting Ti-based matrix composites (TMCs) (Kumar et al., 2017; Li et al., 2020a; Munir et al., 2017; Nan et al., 2004). This is in line with the knowledge that TMCs are gaining more acceptances in industrial applications consequent upon their properties of exceptional strength, high stiffness, and low density (Dong et al., 2020; Jiao et al., 2018; Li et al., 2020b). In addition, TMCs reinforced with MWCNTs have been described as new materials with potential opportunities in industry as they offer outstanding low to moderate density and competitively high elastic modulus (Li et al., 2020a; Zhuang et al., 2020). Although the applications of graphite-reinforced metal matrix composites (MMCs) have attracted much attention lately owing to their superior thermal properties and low cost, the development and characterization of MWCNTs-reinforced TMCs have not received much attention from researchers (Wang et al., 2015). This is despite the understanding that CNTs-reinforced MMCs exhibit improved resistance to thermal fatigue (Bakshi et al., 2010b).

Researchers have attributed this gap to the peculiar processing challenges often encountered in the efforts toward achieving a homogeneous dispersion of the MWCNTs reinforcement within the Ti metal matrix (Adegbenjo et al., 2017a,

2017b; Awotunde et al., 2019; Bakshi et al., 2010a; Li et al., 2013a; Munir et al., 2015a). Other reasons are the requirements for use of elevated sintering temperatures to achieve the full densification of TMCs, as well as the associated possibility of interfacial reactions between Ti metal and defective CNTs at the high processing temperatures (Li et al., 2020a; Munir et al., 2018). Although there are some reported studies available in literature on the thermal behavior of pure Ti matrices reinforced with MWCNTs, there are limited studies reported to date on the thermal characteristics of MWCNTs-reinforced Ti64 metal matrix nanocomposites (MMNCs) to the best of the authors' knowledge, as this group of materials have attracted moderate attention from researchers.

Thus, this current work was undertaken to compensate for this knowledge gap by investigating the effect of MWCNTs contents on the thermal diffusivity characteristics of sintered MWCNTs-reinforced Ti64 (MWCNTs/Ti64) fabricated by spark plasma sintering (SPS), a unique field-assisted sintering technique (FAST). This is built on the foundation from previous studies that small additions of MWCNTs into pure Ti matrix can effectively improve the thermal performance of the resulting TMC and capable of positively expanding the applications of Ti and its alloys (Munir et al., 2017, 2018; Nan et al., 2004; Wang et al., 2015). It is perceived that the results of this present study will aid more research efforts into the applications of high-performance TMC materials as probable replacements for the unreinforced Ti64 in the highly demanding, challenging, unpredictable, and harsh application areas wherein they are mostly employed, especially in the aerospace industries.

## 2 Materials and Methods

### 2.1 Materials

The MWCNTs-reinforced Ti64 nanocomposites in this work were fabricated from pre-alloyed, spherical-shaped Ti64 (average particle size:  $\sim 25 \mu\text{m}$ , procured from TLS Technik GmbH & Co., Germany) and MWCNTs (with outside diameter 20–30 nm, 10–30  $\mu\text{m}$  length, ash content  $<1.5 \text{ wt}\%$  and  $>95 \text{ wt}\%$  purity) powders.

### 2.2 Methods

The as-received MWCNTs were graphitized in a tube furnace (Webb 77 Natick MA, USA) at  $1800 \text{ }^\circ\text{C}$  for 5 h in vacuum before their predetermined quantities were dispersed into the Ti64 metal matrices in a high-energy ball milling (HEBM) machine (Retsch PM 400 MA, Germany) for 6 h at 50 rpm and 10:1 ball-powder ratio (BPR). Both the Ti64 and MWCNTs/Ti64 composite powders containing 1, 2, and 3 wt.%, respectively, of the treated MWCNTs reinforcements were

subsequently consolidated into  $\text{Ø} 40 \text{ mm} \times 5 \text{ mm}$  thickness disks by SPS (HHPD-25, FCT Germany) at different sintering temperatures of 850–1000 °C. Heating rate, holding time, and applied pressure during SPS synthesis were 50 MPa, 5 min, and 100 °C/min, respectively.

Sixteen  $10 \times 10 \times 1 \text{ mm}^3$  test samples for thermal diffusivity experiments were sectioned by precision cutting from the sintered Ti64 and graphitized MWCNTs-reinforced Ti64 nanocomposite disks. The thermal diffusivities of the test samples were measured according to the Laser Flash (LF) (LFA 427 NETZSCH, Germany) method over 50–300 °C temperature range and following the ASTM E1461 procedures. The recorded value for each sample is the mean of three consecutively recorded measurements for each specimen at the specific temperature under consideration. This ensures the reliability, accuracy, and repeatability of all the thermal diffusivity readings collected during the experiments.

As this present study is focused on reporting the influence of added MWCNTs on the thermal characteristics of the sintered bulk MWCNTs-reinforced Ti64 nanocomposites, the details of the parameters used, as well as the processes followed in dispersing MWCNTs into Ti64 metal matrix via HEBM, the subsequent synthesis of the composite powders into bulk composites by SPS, relative density measurements, metallographic preparation, and microstructural analyses of the samples, are not stated in this present paper; these have been adequately reported elsewhere (Adegbenjo et al., 2017b, 2018).

### 3 Results and Discussion

#### 3.1 *Microstructural Evolution and Densification of the Fabricated Samples*

The microstructural evolution and densification pattern in sintered unreinforced Ti64 and MWCNTs/Ti64 nanocomposites is brought up here in this current study because it will be needed to fully discuss the thermal behavior of the consolidated bulk nanocomposites. The subject has been dealt with in detail elsewhere (Adegbenjo et al., 2017b, 2018). Figure 13.1 shows the secondary electron images (SEI) of the sintered unreinforced Ti64 and MWCNTs/Ti64 nanocomposites consolidated at 1000 °C as observed from the SEM analyses of the samples. The unreinforced Ti64 alloy as seen in Fig. 13.1a shows the typical fully lamellar structure of Ti64 alloy with the characteristic basket weave (Widmanstätten)  $\alpha + \beta$  network. However, it was observed that the addition of MWCNTs to Ti64 matrices resulted in transforming this characteristic structure from fully lamellar to equiaxed as could be seen in Fig. 13.1b–d for the sintered nanocomposite samples. All the consolidated samples were sintered to full densification; hence, there were no significant pores observed in the presented images. However, re-agglomerated MWCNTs (shown by black arrows) and TiC (indicated by blue arrows) resulting from the interfacial reaction

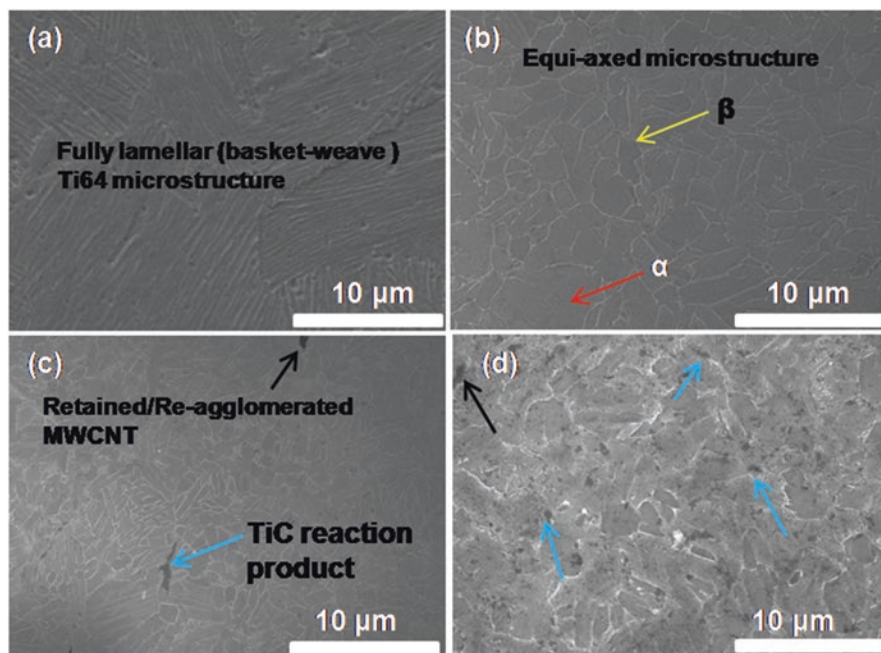


**Fig. 13.1** Micrographs of sintered (a) unreinforced Ti64 and MWCNTs-reinforced Ti64 nanocomposites containing varied MWCNTs reinforcements (b) 1 wt.%, (c) 2 wt.%, and (d) 3 wt.%; all consolidated at 1000 °C by SPS

between defective MWCNTs and Ti64 metal particles were observed in the composite samples containing 2 and 3 wt.% MWCNTs, respectively (Fig. 13.1c, d). The 3 wt.% MWCNTs/Ti64 composite exhibited higher TiC content as seen in Fig. 13.1d, which suggests that the composite had more re-agglomerated and damaged CNTs that reacted with Ti64 particles to form the interfacial products (Adegbenjo et al., 2018). This is because the tendency to homogeneously disperse MWCNTs within the alloy matrix becomes increasingly difficult with a higher content of the reinforcement within it (Adegbenjo et al., 2017a, 2019b).

The densification in the unreinforced Ti64 and MWCNTs/Ti64 nanocomposites consolidated by SPS at different sintering temperatures (850–1000 °C) are as shown in Fig. 13.2. Although the unreinforced Ti64 sample reached almost theoretical densities at all the investigated sintering temperatures, it was observed that composite densities reduced steadily with the addition of increasing weight fractions of MWCNTs to Ti64 matrices. Nevertheless, a similar trend of improved densification was seen in both the unreinforced Ti64 and composite samples as the sintering temperature was increased from 850 to 1000 °C. Previous studies have attributed the deteriorating relative densities with the addition of MWCNTs to the presence of re-agglomerated and clustered MWCNTs in the Ti64 metal matrix. Poor interfacial bonding within the composites as a result of insufficient diffusion between Ti64 and

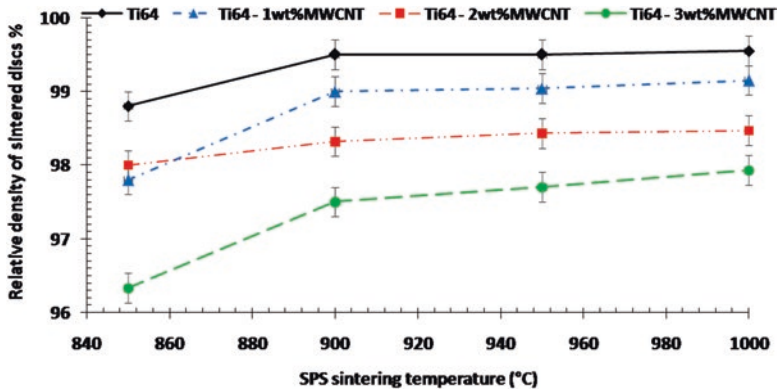


**Fig. 13.2** Relative densities of sintered unreinforced Ti64 and MWCNTs reinforced Ti64 nanocomposites at varied sintering temperatures (Adegbenjo et al., 2017b)

the MWCNTs could also cause thermal gradients between the metal matrix and the MWCNTs reinforcement, and this most probably culminated in the declining densification in the composites (Adegbenjo et al., 2017b). On the other hand, the observed enhancements in relative densities with increasing sintering temperatures was attributed to the presumed increased diffusion bonding and atom mobility expectedly with higher sintering temperatures (Adegbenjo et al., 2017b, 2018). These results are in agreement with the outcomes of reported studies on the reinforcement of Al and Ti metal matrices with MWCNTs wherein the authors submitted that even small amounts of CNTs in a metal matrix is sufficient to cause a decline in the relative densities of the resulting composites (Saheb, 2014; Wang et al., 2015). However, the composites with 1 wt.% MWCNTs content had better relative densities compared to the other composites, presumably due to the better dispersion of the MWCNTs in this sample as seen in Fig. 13.1b.

### 3.2 Thermal Diffusivity Characteristics of Ti64 Alloy and MWCNTs/Ti64 Nanocomposites

The thermal diffusivities of the unreinforced Ti64 and MWCNTs/Ti64 nanocomposites synthesized at varying temperatures are as represented in Fig. 13.3. For the samples consolidated at 850 °C (Fig. 13.3a), the addition of 1 and 2 wt.% MWCNTs, respectively, to Ti64 matrix enhanced the measured thermal diffusivities of the consolidated nanocomposites over that of the virgin Ti64 samples at all the temperatures (50–300 °C) under which the thermal diffusivities were investigated. Considering the two extremes of the testing temperatures, it was observed that at 50 °C, the measured thermal diffusivities of the nanocomposites were improved by 1.7 and 14% with the addition of 1 and 2 wt.% MWCNTs to Ti64, respectively, over the recorded values for the unreinforced alloy, while 4 and 9% improvements were

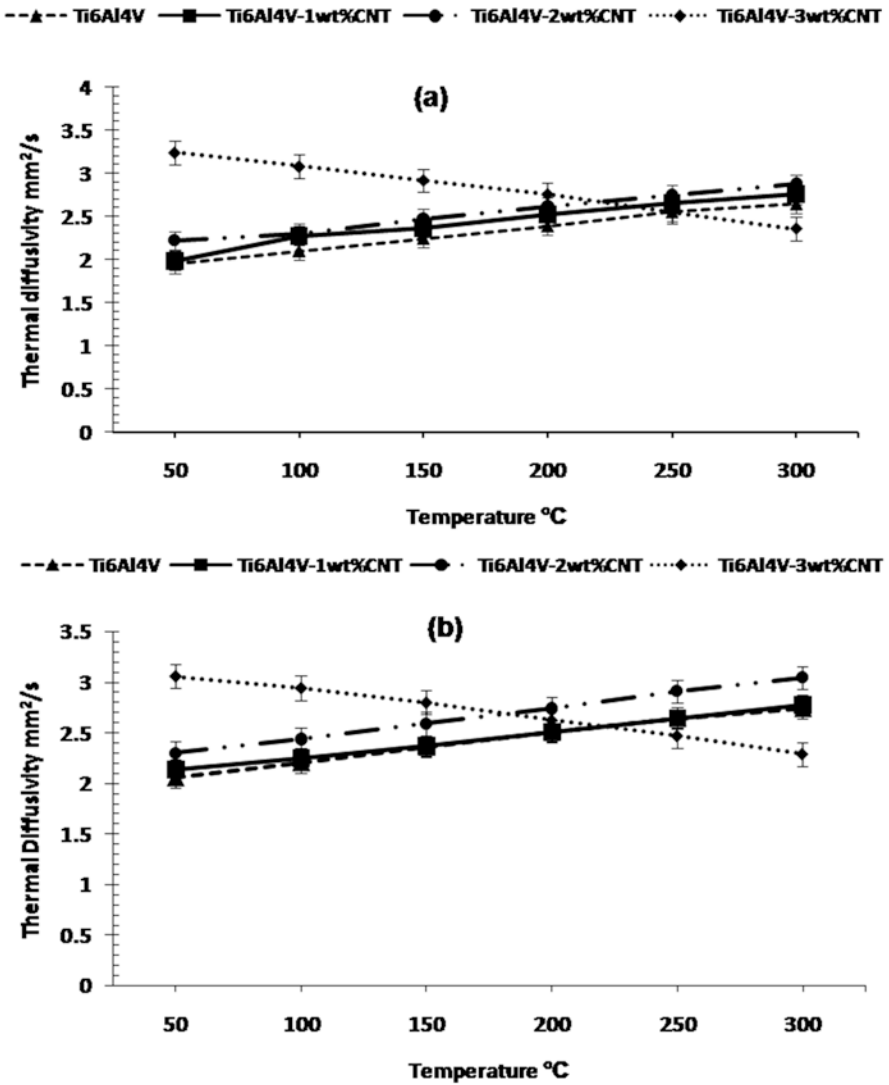


Fig. 13.3 Recorded thermal diffusivities of Ti64 and MWCNTs-reinforced Ti64 nanocomposites sintered at different temperatures (a) 850 °C, (b) 900 °C, (c) 950 °C, and (d) 1000 °C

recorded at 300 °C for the same amounts of MWCNTs added to Ti64 metal matrices, respectively. However, with the addition of 3 wt.% MWCNTs to Ti64, a completely different and opposite trend in the thermal diffusivity behavior of the consolidated nanocomposites was observed. Although the measured diffusivities of the 3 wt.% composites were initially better, compared to the other samples with 1 and 2 wt.% of added MWCNTs reinforcements, respectively, from 50 °C up to

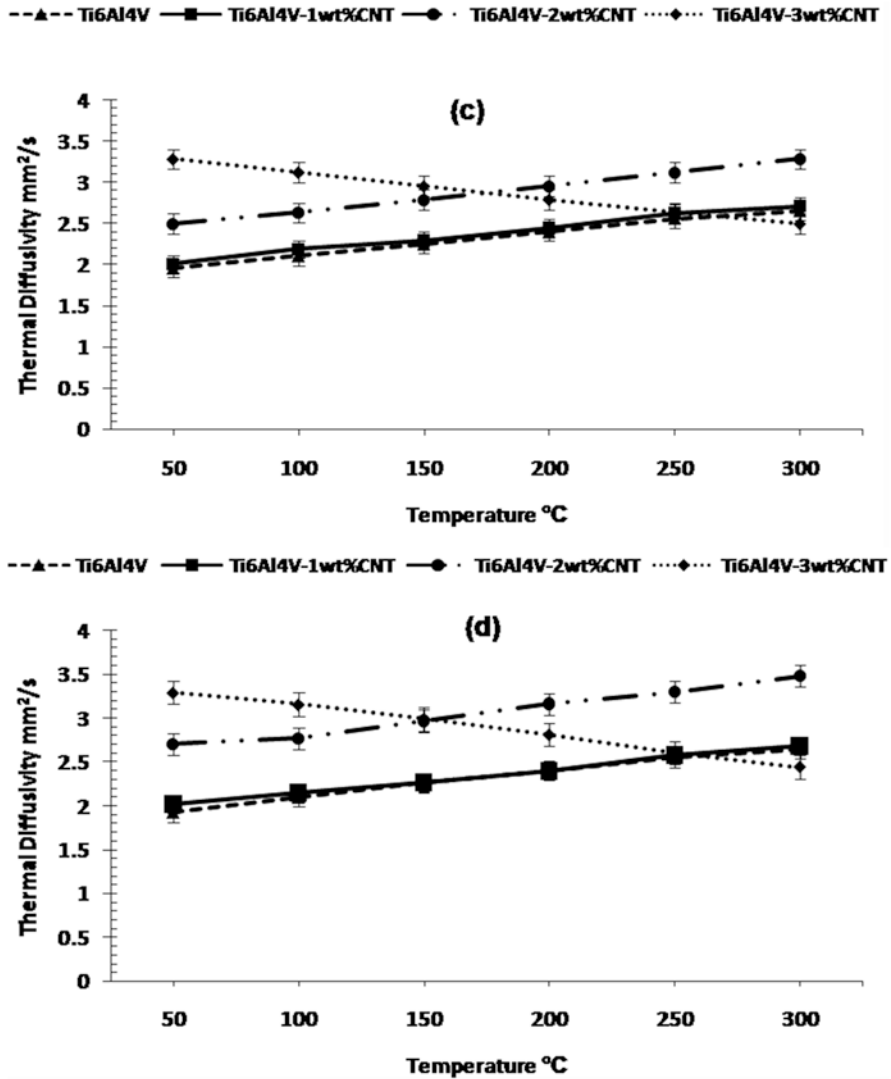


Fig. 13.3 (continued)

200 °C, its recorded thermal diffusivities continued to drop progressively as the testing temperatures investigated were increased. This occurred such that the value recorded for this composite was below that of the unreinforced Ti64 alloy between 250 and 300 °C. Thus, the thermal diffusivities of the 3 wt.% composite deteriorated from 3.24 mm<sup>2</sup>/s at 50 °C to 2.36 mm<sup>2</sup>/s at 300 °C, implying 27% degradation in the recorded thermal diffusivity of the composite. However, comparing the 3 wt.% MWCNTs nanocomposite with the unreinforced Ti64 sample, thermal diffusivities



of 3.24 and 1.95 mm<sup>2</sup>/s, respectively, were recorded at 50 °C while 2.36 and 2.65 mm<sup>2</sup>/s, respectively, were recorded at 300 °C.

This implies that although the 3 wt.% composite exhibited an enhancement in thermal diffusivity of 66% over unreinforced Ti64 at 50 °C, a depreciation of 11% in the observed diffusivity value was obtained at 300 °C with respect to the unreinforced matrix alloy. In essence, the 3 wt.% composite lost 55% of the enhancement it gained initially at 50 °C over Ti64, as the testing temperature was raised from 50 °C through 300 °C. This shows that despite the fact that the thermal diffusivity performance of the 3 wt.% MWCNTs nanocomposite was the best at lower temperatures compared to the other composites, its performance deteriorates at higher temperatures to the point of falling under that of the unreinforced alloy, which suggests this composite will not be suitable for high-temperature applications. A similar trend in thermal diffusivity behaviors was observed in Fig. 13.3b–d for the other samples sintered at temperatures of 900–1000 °C, respectively, except that the recorded thermal diffusivities of the 3 wt.% MWCNTs composites started to drop below that of the 2 wt.% composite at 200 °C, instead of 250 °C observed earlier at 850 °C sintering temperature.

The noticed decline in the thermal diffusivity behavior of the 3 wt.% MWCNTs composite was attributed to the agglomeration and re-agglomeration of the MWCNTs (i.e., during powder dispersion and sintering, respectively) within the composite arising from the increased difficulty in separating them to achieve their adequate homogeneous dispersion within the Ti64 metal at higher contents of MWCNTs. This difficulty is partly as a result of the high aspect ratio of the MWCNTs, their inherent nano-size dimensions and large surface area. The other factors responsible for this are the tubular morphology of the nanotubes and the strong van der Waals forces in the individual tubes which become predominantly higher with increased contents of the added MWCNTs reinforcement in the metal matrix (Liu et al., 2020; Munir et al., 2015b, 2016; Thostenson et al., 2001). The tendency to losing the positive impact of the MWCNTs reinforcement is also increased at higher contents owing to the amorphization of the MWCNTs which arises from the energy absorbed by them during their dispersion processing by milling, either from the milling balls or friction among the nanotubes and their neighboring Ti particles. This leads to a degeneration of the highly graphitic sp<sup>2</sup> C-C network into the highly reactive and amorphous sp<sup>3</sup> C-C phases in the MWCNTs, which subsequently forms TiC interfacial reaction products, when these defective MWCNTs react with Ti64 particles as seen in Fig. 13.1d (Adegbenjo et al., 2017b; Ferrari & Robertson, 2000; Lespade et al., 1984; Munir et al., 2015c). The channels of defects or damages introduction into carbonaceous materials as identified in literature are via bond angle disorder, bond length disorder, and hybridization, while a three-stage model for a typical amorphization trajectory was put forth as: from graphite to nanocrystalline graphite to amorphous carbon to tetrahedral amorphous carbon (Ferrari, 2007; Ferrari & Robertson, 2000; Lespade et al., 1984).

Hence, the diffusivities of the MWCNTs/Ti64 samples suggest the enhancement in the diffusivity Ti64 is predominantly a contribution of the extent of MWCNTs reinforcement dispersion within its particles. This outcome is in total conformity

with reports of Wang et al., on the diffusivities of pure Ti matrices reinforced with MWCNTs (Wang et al., 2015). They advanced that the observed diffusivities of SPS MWCNTs/Ti samples were enhanced steadily with increase in the fractions of added reinforcement contents in a declining growth rate order. This present investigation also reveals that the diffusivity characteristics of the synthesized nanocomposites is not dependent on the densities of the consolidated samples as the 2 wt.% samples with increased MWCNTs wt.% exhibited improved diffusivities notwithstanding their relatively lower densities compared to the 1 wt.% composites. This is most probably because thermal diffusivity is not only a function of the thickness of the samples and heat diffusion time but also of temperature, which is not dependent on the density of the samples. This explains why the observed thermal diffusivities of the composites in this work were better at higher temperatures, suggesting that the investigated parameter was dependent on thermal transport mechanisms which are based on phonon diffusion in the metal matrix and ballistic transportation in the MWCNTs reinforcement (Wang et al., 2015). It is perceived that this thermal transport must have been hampered in the 3 wt.% composites leading to the observed diminishing thermal diffusivities in these samples at higher temperatures. The inherent pores occurring from increased possibility of nanotubes to get agglomerated as presented in Fig. 13.1d may also be responsible for this, as the pores could act as thermal barriers to effective heat flow in the composites and consequently affect their diffusivities adversely (Song & Youn, 2006; Wang et al., 2013).

The overall thermal diffusivity enhancement in the 2 wt.% MWCNTs composites on one hand is thought to be due to the comparatively lower weight fraction of reinforcement which promoted a relatively better dispersion of the MWCNTs and higher ballistic transportation capacity in the sample. On the other hand, the presence of moderate TiC (Fig. 13.1c) must have contributed positively to the observed improved thermal diffusivity behavior of this sample. This may be supported from the fact that reaction products such as carbides formed during the reaction between defective CNTs, and metal particles are capable of improving the composite wettability through reactive wetting (Bakshi et al., 2009; Laha et al., 2007; Landry et al., 1997). Although the 3 wt.% MWCNTs composite had more TiC reaction products as seen in Fig. 13.1d, these could not positively sustain enhanced thermal diffusivity at higher temperatures due to perceived weak or entirely poor bonding between the TiC and the surrounding Ti64 metal matrix which possibly made the composite structure unstable at the TiC/matrix interface (Li et al., 2020a). This is not far-fetched as a previous study by Bakshi et al. opined that reaction products at composite interfaces may or may not be supportive of a composite's overall thermal properties depending on whether they increase or decrease the CNTs/matrix thermal conductance (Bakshi et al., 2010b).

This perceived varied contribution to thermal diffusivity performance by TiC presence in the consolidated composites from this current study is not strange as the role played (whether positive or negative) by TiC reaction products on the overall bulk TMCs properties has remained a controversial issue and a subject of debate up till date (Adegbenjo et al., 2019b). For instance, some reported studies posited that

TiC formed in situ contributes dispersion strengthening to Ti matrix, while others insisted that the chemical reaction resulting in TiC formation is capable of subsequently damaging the CNTs structure, therefore adversely impacting the properties of the bulk composite (Munir et al., 2015b; Munir & Wen, 2016; Wang et al., 2015). Wang et al. (2015) claimed that TiC's absence in CNTs-reinforced TMCs does not have a specific effect on the interfacial bond strength of the composite, whereas Azarniya et al. (2017) and Kondoh et al. (2012) reported that although TiC phases may aid effective interfacial bonding in MWCNTs/Ti composites at low temperatures, they could adversely affect composite properties at elevated temperatures. A more recent study by Li et al. (2020a) in support of the foregoing also posited that the TiC formed during the SPS processing of CNTs reinforced TMCs can have either a positive or negative influence on the overall property of the TMCs. Furthermore, another much recent study by Li et al. (2020b) in explaining the controversy around the role of TiC reaction products in MWCNTs/TMCs submitted that the process of TiC formation and its position (either on the interface or intragranular) within the composite structure determine whether the formed carbide will play a positive role in the bulk composite or otherwise. They investigated the formation of two types of TiC when 0.25 wt.% CNTs was added to Ti64 matrix powder and consolidated by SPS at 800 °C for 5 min. They attributed the formation of TiC nanoparticles to the in situ interfacial reaction between CNTs and Ti64 metal matrix. It was further stated that a significant amount of the TiC nanoplatelets must have been formed within the grains at 800 °C, suggesting that the inward diffusion of amorphous carbon (a-C) into Ti64 took place long before the occurrence of Ti/CNTs interfacial reaction. Hence, the reported study concluded that the CNTs and the formed TiC nanoparticles were distributed along the grain boundaries while the TiC nanoplatelets were mostly distributed homogeneously within the intragranular microstructure of the bulk composite.

From the foregoing therefore, it may be instructive to submit from this present study that the formed TiCs seen in Fig. 13.1c, d are most plausibly intragranular and interfacial, respectively, based on their presumed roles on the exhibited thermal diffusivities of the synthesized composites. This position conforms to the opinions presented in reported studies that a larger proportion of the carbide reinforcements in TMCs prepared by the powder metallurgy (P/M) route are mostly distributed along the grain boundaries, with a few of them found within the grains, which at times compromises the property enhancement expected of the synthesized bulk composite (Chen et al., 2017; Hayat et al., 2019; Li et al., 2013b; Munir et al., 2015b, 2018; Zheng et al., 2016). This proposition is absolutely in agreement with the reports from the work of Wang et al. (2015) and our previous studies on SPS-processed MWCNTs/Ti64 composites, wherein it was posited that polycrystalline layers of TiC reaction products were formed between Ti64 metal particles and MWCNTs clusters which were mostly situated on the Ti grain boundaries (Adegbenjo et al., 2018, 2019b).

### 3.3 Thermal Conductivity of MWCNTs/Ti64 Nanocomposites

It is a universal understanding that the thermal conductivity behavior of a sample is a reflection of its thermal diffusivity characteristics, as there is a direct relationship between the two quantities. Bakshi et al. (2010b) have established this in their previous study on the thermal conductivity of carbon nanotube-reinforced aluminium (CNTs/Al) composites using the object-oriented finite element method. The universally established and accepted relationship between these quantities is stated in Eq. (13.1), where  $k$  is the thermal conductivity,  $\alpha$  is thermal diffusivity,  $\rho$  is the density of the sample, and  $C_p$  is specific heat capacity.

$$k = \alpha \times \rho \times C_p \quad (13.1)$$

Thus, it is presumed from the outcome of this work that the thermal conductivity of the synthesized bulk nanocomposites will generally be better than that of the unreinforced Ti64 matrix alloy because of the added MWCNTs in the composites. It is also expected that the thermal conductivity of the 3 wt.% MWCNTs will deteriorate at higher temperatures in comparison with the other composites in the same pattern as observed for the thermal diffusivity behavior of the nanocomposites. This position is based on the reported outcomes obtained from previous similar studies by different researchers. For instance, Wang et al. (2015), showed that CNTs agglomeration in MWCNTs reinforced pure Ti metal matrices resulted in the degradation of the thermal conductivity of the composites with higher wt.% of MWCNTs. They attributed this to three reasons, which are (1) increased possibility of random nanotubes orientation as a result of aggregating individual tubes into clusters, (2) reduced thermal diffusivity in the composites due to the presence of pores at the MWCNTs-Ti interfaces and among the nanotubes, consequent upon the aggregation of the MWCNTs. These pores were thought to be capable of effectively spreading heat flow, with those pores at the interfaces constituting themselves as thermal barriers, and (3) the thermal conductivity of the composites is adversely impacted with aggregated MWCNTs, due to the reduction in the cleaning effect during SPS processing arising from weakened spark discharge effects, as the cleaning effect not only reduces kinks and twists in MWCNTs but also eliminates impurities and contaminations present in them (Chu et al., 2010b; Kumari et al., 2008; Sivakumar et al., 2007). Other reported works are also in agreement with this position by submitting that agglomeration of CNTs will reduce the heat conduction performance in CNTs-reinforced metal/polymer matrix composites (Song & Youn, 2006; Wang et al., 2013).

The 2 wt.% MWCNTs composite is again expected to exhibit the best thermal conductivity among the composites in this study, notwithstanding the better densification of the 1 wt.% MWCNTs composite (Fig. 13.2), just as the former had better thermal diffusivities as seen earlier. Intuitively, one may want to contest this, especially with the additional understanding that thermal conductivity is a function of the sample's density. However, a reported similar study by Chih-Jong et al., had laid

this contention to rest having shown in their work that the thermal conductivity of graphite-reinforced aluminium matrix composites increased despite decreasing densities of the composites with increasing volume fractions of the graphite reinforcement in the metal matrix (Chih-Jong et al., 2009). The presence of suspected intragranular TiC interfacial products having a healthy and strong bonding with the surrounding Ti particles must have promoted the presumed improvement in thermal conductivity expected of the 2 wt.% MWCNTs composite (Li et al., 2020b), as against the weakly bonded interfacial or grain boundary TiC in the 3 wt.% MWCNTs composite. This is consistent with the fact that a weak interface promotes the formation of porosity which will, of course, adversely affect the conductivity performance of the composite. This is because porosity between individual CNTs results in compromised interfacial heat transfer and consequently reduces the thermal conductivity capacity of the bulk CNTs-reinforced composite (Bakshi et al., 2010b). Furthermore, reported works have also submitted that the interface in CNTs/MMCs plays a crucial part in dictating the properties of the bulk composite as the quality of the interface formed is dependent on the wetting ability of the CNTs, their structural integrity, the prevalent interface reactions, and the extent of carbide formation (Baig et al., 2016). This position was supported by Hamamda et al. (2017) that weak bonds in Cu-CNTs interfaces were responsible for the limited heat flow and reduced thermal conductivity reported in these composites. Hence, the integrity of the interface and its strength is critical for adequate composite strength and exceptional performance (Adegbenjo et al., 2019b; Baig et al., 2016; Ke & Chengchang, 2014). In addition, Chu et al. (2010a) and Hu et al. (2018) agreed that the presence of kinks and twists (due to CNTs clustering, agglomeration, and re-agglomeration), which are unavoidable with higher CNTs weight percents in a metal matrix, is bound to deteriorate the thermal conductivity of the synthesized composite. This was exhibited by the 3 wt.% MWCNTs composites in this current study, which is consistent with the previously reported findings of Song et al. (2006) that smaller CNTs length efficiencies are supportive of improved thermal conductivity, as the effective length of long CNTs are reduced with the presence of kinks and twists, curves, or bends in the nanotubes.

## 4 Conclusion

This study investigated the influence of added graphitized MWCNTs on the thermal characteristics of carbon nanotube-reinforced Ti64 nanocomposites synthesized by the SPS technique. The addition of MWCNTs to Ti64 improved the thermal diffusivity performance of the synthesized bulk nanocomposites. It was observed that achieving the positive impact of the added MWCNTs was dependent on the extent of MWCNTs dispersion within the metal matrix, the strength and integrity of the composite interface, and the role played by TiC reaction products formed due to the reaction between the Ti metal particles and amorphous carbon (a-C) from defective MWCNTs. Overall, the 2 wt.% MWCNTs composite exhibited the best thermal

characteristics of the synthesized nanocomposites due to the presumed synergistic effects of comparatively homogeneous MWCNTs dispersion and suspected intra-granular TiC which had strong bonding with the surrounding Ti64 particles in this composite. It is expected that the outcome of this study will open new grounds in the application of MWCNTs/Ti64 nanocomposites materials for wing box and fuselage fabrications in the aerospace industries.

**Acknowledgments** The authors would like to appreciate the University of Johannesburg, South Africa, for the financial support toward this work. The Institute for NanoEngineering Research, Tshwane University of Technology, Pretoria 0001, South Africa, is also appreciated for allowing us to use the Laser Flash equipment for the experiments in the course of this study.

**Conflict of Interest** The authors declare that there are no conflicts of interest involved in this work.

## References

- Adegbenjo, A., Obadele, B., Olubambi, P., Shongwe, M., & Adejuwon, S. (2019a). Thermal diffusivity behaviour of multi-walled carbon nanotube reinforced Ti6Al4V metal matrix composites. *IOP Conference Series: Materials Science and Engineering*, 499, 012002. <https://doi.org/10.1088/1757-899x/499/1/012002>
- Adegbenjo, A. O., Obadele, B. A., & Olubambi, P. A. (2018). Densification, hardness and tribological characteristics of MWCNTs reinforced Ti6Al4V compacts consolidated by spark plasma sintering. *Journal of Alloys and Compounds*, 749, 818–833. <https://doi.org/10.1016/j.jallcom.2018.03.373>
- Adegbenjo, A. O., Olubambi, P. A., Potgieter, J. H., Nsiah-Baafi, E., & Shongwe, M. B. (2017a). Interfacial reaction during high energy ball milling dispersion of carbon nanotubes into Ti6Al4V. *Journal of Materials Engineering and Performance*, 26(12), 6047–6056. <https://doi.org/10.1007/s11665-017-3041-8>
- Adegbenjo, A. O., Olubambi, P. A., Potgieter, J. H., Shongwe, M. B., & Ramakokovhu, M. (2017b). Spark plasma sintering of graphitized multi-walled carbon nanotube reinforced Ti6Al4V. *Materials & Design*, 128, 119–129. <https://doi.org/10.1016/j.matdes.2017.05.003>
- Adegbenjo, A. O., Olubambi, P. A., Westraadt, J. E., Lesufi, M., & Mphahlele, M. R. (2019b). Interface analysis of spark plasma sintered carbon nanotube reinforced Ti6Al4V. *JOM*, 71(7), 2262–2271. <https://doi.org/10.1007/s11837-019-03476-x>
- Awotunde, M. A., Adegbenjo, A. O., Ayodele, O. O., Okoro, A. M., Shongwe, M. B., & Olubambi, P. A. (2019). Interdependence of carbon nanotubes agglomerations, its structural integrity and the mechanical properties of reinforced nickel aluminide composites. *Journal of Alloys and Compounds*, 803, 514–526. <https://doi.org/10.1016/j.jallcom.2019.06.297>
- Azarniya, A., Azarniya, A., Sovizi, S., Hosseini, H. R. M., Varol, T., Kawasaki, A., & Ramakrishna, S. (2017). Physicomechanical properties of spark plasma sintered carbon nanotube-reinforced metal matrix nanocomposites. *Progress in Materials Science*, 90, 276–324.
- Babapoor, A., Asl, M. S., Ahmadi, Z., & Namini, A. S. (2018). Effects of spark plasma sintering temperature on densification, hardness and thermal conductivity of titanium carbide. *Ceramics International*, 44(12), 14541–14546. <https://doi.org/10.1016/j.ceramint.2018.05.071>
- Baig, Z., Mamat, O., & Mustapha, M. (2016). Recent progress on the dispersion and the strengthening effect of carbon nanotubes and graphene-reinforced metal nanocomposites: A review. *Critical Reviews in Solid State and Materials Sciences*, 1–46.
- Bakshi, S., Lahiri, D., & Agarwal, A. (2010a). Carbon nanotube reinforced metal matrix composites—a review. *International Materials Reviews*, 55(1), 41–64.

- Bakshi, S. R., Keshri, A. K., Singh, V., Seal, S., & Agarwal, A. (2009). Interface in carbon nanotube reinforced aluminum silicon composites: Thermodynamic analysis and experimental verification. *Journal of Alloys and Compounds*, 481(1), 207–213. <https://doi.org/10.1016/j.jallcom.2009.03.055>
- Bakshi, S. R., Patel, R. R., & Agarwal, A. (2010b). Thermal conductivity of carbon nanotube reinforced aluminum composites: A multi-scale study using object oriented finite element method. *Computational Materials Science*, 50(2), 419–428. <https://doi.org/10.1016/j.commatsci.2010.08.034>
- Bhat, A., Balla, V. K., Bysakh, S., Basu, D., Bose, S., & Bandyopadhyay, A. (2011). Carbon nanotube reinforced Cu–10Sn alloy composites: Mechanical and thermal properties. *Materials Science and Engineering: A*, 528(22), 6727–6732.
- Chen, B., Shen, J., Ye, X., Jia, L., Li, S., Umeda, J., Takahashi, M., & Kondoh, K. (2017). Length effect of carbon nanotubes on the strengthening mechanisms in metal matrix composites. *Acta Materialia*, 140, 317–325. <https://doi.org/10.1016/j.actamat.2017.08.048>
- Chih-Jong, C., Chih-Hao, C., Jen-Dong, H., & Cheng-Tzu, K. (2009). Thermal characterization of high thermal conductive graphites reinforced aluminum matrix composites. In *2009 4th International Microsystems, Packaging, Assembly and Circuits Technology Conference*, 21–23 Oct. 2009 (pp. 461–464). <https://doi.org/10.1109/IMPACT.2009.5382217>
- Chu, K., Guo, H., Jia, C., Yin, F., Zhang, X., Liang, X., & Chen, H. (2010a). Thermal properties of carbon nanotube–copper composites for thermal management applications. *Nanoscale Research Letters*, 5(5), 868. <https://doi.org/10.1007/s11671-010-9577-2>
- Chu, K., Wu, Q., Jia, C., Liang, X., Nie, J., Tian, W., Gai, G., & Guo, H. (2010b). Fabrication and effective thermal conductivity of multi-walled carbon nanotubes reinforced Cu matrix composites for heat sink applications. *Composites Science and Technology*, 70(2), 298–304. <https://doi.org/10.1016/j.compscitech.2009.10.021>
- Dong, L. L., Lu, J. W., Fu, Y. Q., Huo, W. T., Liu, Y., Li, D. D., & Zhang, Y. S. (2020). Carbonaceous nanomaterial reinforced Ti-6Al-4V matrix composites: Properties, interfacial structures and strengthening mechanisms. *Carbon*, 164, 272–286. <https://doi.org/10.1016/j.carbon.2020.04.009>
- Ferrari, A. C. (2007). Raman spectroscopy of graphene and graphite: Disorder, electron–phonon coupling, doping and nonadiabatic effects. *Solid State Communications*, 143(1–2), 47–57. <https://doi.org/10.1016/j.ssc.2007.03.052>
- Ferrari, A. C., & Robertson, J. (2000). Interpretation of Raman spectra of disordered and amorphous carbon. *Physical Review B*, 61(20), 14095.
- Hamamda, S., Jari, A., Revo, S., Ivanenko, K., Jari, Y., & Avramenko, T. (2017). Thermal analysis of copper-titanium-multiwall carbon nanotube composites. *Nanoscale Research Letters*, 12(1), 251. <https://doi.org/10.1186/s11671-017-2025-9>
- Hayat, M. D., Singh, H., He, Z., & Cao, P. (2019). Titanium metal matrix composites: An overview. *Composites Part A: Applied Science and Manufacturing*, 121, 418–438. <https://doi.org/10.1016/j.compositesa.2019.04.005>
- Hu, W., Zhao-Hui, Z., Zheng-Yang, H., Qi, S., & Shi-Pan, Y. (2018). Interface structure and properties of CNTs/Cu composites fabricated by electroless deposition and spark plasma sintering. *Materials Research Express*, 5(1), 015602.
- Inagaki, I., Takechi, T., & Ariyasu, Y. S. N. (2014). *Application and features of titanium for the aerospace industry*.
- Işik, B., & Kentli, A. (2014). The prediction of surface temperature in drilling of Ti6Al4V. *Archives of Metallurgy and Materials*, 59(2), 467–471.
- Jiao, Y., Huang, L., & Geng, L. (2018). Progress on discontinuously reinforced titanium matrix composites. *Journal of Alloys and Compounds*, 767, 1196–1215. <https://doi.org/10.1016/j.jallcom.2018.07.100>
- Ke, C., & Chengchang, J. (2014). Enhanced strength in bulk graphene–copper composites. *Physica Status Solidi (A)*, 211(1), 184–190. <https://doi.org/10.1002/pssa.201330051>

- Kondoh, K., Threrujirapong, T., Umeda, J., & Fugetsu, B. (2012). High-temperature properties of extruded titanium composites fabricated from carbon nanotubes coated titanium powder by spark plasma sintering and hot extrusion. *Composites Science and Technology*, 72(11), 1291–1297.
- Kumar, M. N., Mahmoodi, M., TabkhPaz, M., Park, S. S., & Jin, X. (2017). Characterization and micro end milling of graphene nano platelet and carbon nanotube filled nanocomposites. *Journal of Materials Processing Technology*, 249, 96–107. <https://doi.org/10.1016/j.jmatprotec.2017.06.005>
- Kumari, L., Zhang, T., Du, G. H., Li, W. Z., Wang, Q. W., Datye, A., & Wu, K. H. (2008). Thermal properties of CNT-Alumina nanocomposites. *Composites Science and Technology*, 68(9), 2178–2183. <https://doi.org/10.1016/j.compscitech.2008.04.001>
- Laha, T., Kuchibhatla, S., Seal, S., Li, W., & Agarwal, A. (2007). Interfacial phenomena in thermally sprayed multiwalled carbon nanotube reinforced aluminum nanocomposite. *Acta Materialia*, 55(3), 1059–1066. <https://doi.org/10.1016/j.actamat.2006.09.025>
- Landry, K., Rado, C., Voitovich, R., & Eustathopoulos, N. (1997). Mechanisms of reactive wetting: the question of triple line configuration. *Acta Materialia*, 45(7), 3079–3085. [https://doi.org/10.1016/S1359-6454\(96\)00372-2](https://doi.org/10.1016/S1359-6454(96)00372-2)
- Lephuthing, S. S., Okoro, A. M., Ige, O. O., & Olubambi, P. A. (2020). Exploring the sintering and densification behaviour of multiwalled carbon nanotube reinforced TiO<sub>2</sub>-MnO<sub>2</sub> composites developed by spark plasma sintering. *Journal of Alloys and Compounds*, 835, 155393. <https://doi.org/10.1016/j.jallcom.2020.155393>
- Lespade, P., Marchand, A., Couzi, M., & Cruege, F. (1984). Caraceterisation de materiaux carbonés par microspectrometrie Raman. *Carbon*, 22(4–5), 375–385.
- Li, G., Munir, K., Wen, C., Li, Y., & Ding, S. (2020a). Machinability of titanium matrix composites (TMC) reinforced with multi-walled carbon nanotubes. *Journal of Manufacturing Processes*, 56, 131–146. <https://doi.org/10.1016/j.jmapro.2020.04.008>
- Li, S., Sun, B., Imai, H., & Kondoh, K. (2013a). Powder metallurgy Ti–TiC metal matrix composites prepared by in situ reactive processing of Ti-VGCFs system. *Carbon*, 61, 216–228.
- Li, S., Sun, B., Imai, H., Mimoto, T., & Kondoh, K. (2013b). Powder metallurgy titanium metal matrix composites reinforced with carbon nanotubes and graphite. *Composites Part A: Applied Science and Manufacturing*, 48, 57–66.
- Li, S., Yang, Y., Misra, R. D. K., Liu, Y., Ye, D., Hu, C., & Xiang, M. (2020b). Interfacial/intragranular reinforcement of titanium-matrix composites produced by a novel process involving core-shell structured powder. *Carbon*, 164, 378–390. <https://doi.org/10.1016/j.carbon.2020.04.010>
- Liu, Y., Li, S., Misra, R. D. K., Geng, K., & Yang, Y. (2020). Planting carbon nanotubes within Ti-6Al-4V to make high-quality composite powders for 3D printing high-performance Ti-6Al-4V matrix composites. *Scripta Materialia*, 183, 6–11. <https://doi.org/10.1016/j.scriptamat.2020.03.009>
- Munir, K. S., Kingshott, P., & Wen, C. (2015a). Carbon nanotube reinforced titanium metal matrix composites prepared by powder metallurgy—A review. *Critical Reviews in Solid State and Materials Sciences*, 40(1), 38–55.
- Munir, K. S., Li, Y., Liang, D., Qian, M., Xu, W., & Wen, C. (2015b). Effect of dispersion method on the deterioration, interfacial interactions and re-agglomeration of carbon nanotubes in titanium metal matrix composites. *Materials & Design*, 88, 138–148.
- Munir, K. S., Li, Y., Lin, J., & Wen, C. (2018). Interdependencies between graphitization of carbon nanotubes and strengthening mechanisms in titanium matrix composites. *Materialia*, 3, 122–138. <https://doi.org/10.1016/j.mtla.2018.08.015>
- Munir, K. S., Li, Y., Qian, M., & Wen, C. (2016). Identifying and understanding the effect of milling energy on the synthesis of carbon nanotubes reinforced titanium metal matrix composites. *Carbon*, 99, 384–397.
- Munir, K. S., Qian, M., Li, Y., Oldfield, D. T., Kingshott, P., Zhu, D. M., & Wen, C. (2015c). Quantitative analyses of MWCNT-Ti powder mixtures using Raman spectroscopy: The influ-



- ence of milling parameters on nanostructural evolution. *Advanced Engineering Materials*, 17(11), 1660–1669.
- Munir, K. S., & Wen, C. (2016). Deterioration of the strong sp<sup>2</sup> carbon network in carbon nanotubes during the mechanical dispersion processing—A review. *Critical Reviews in Solid State and Materials Sciences*, 41(5), 347–366.
- Munir, K. S., Zheng, Y., Zhang, D., Lin, J., Li, Y., & Wen, C. (2017). Improving the strengthening efficiency of carbon nanotubes in titanium metal matrix composites. *Materials Science and Engineering: A*, 696, 10–25. <https://doi.org/10.1016/j.msea.2017.04.026>
- Nan, C.-W., Liu, G., Lin, Y., & Li, M. (2004). Interface effect on thermal conductivity of carbon nanotube composites. *Applied Physics Letters*, 85(16), 3549–3551. <https://doi.org/10.1063/1.1808874>
- Saheb, N. (2014). Sintering behavior of CNT reinforced Al6061 and Al2124 nanocomposites. *Advances in Materials Science and Engineering*, 2014, 1–9.
- Sivakumar, R., Guo, S., Nishimura, T., & Kagawa, Y. (2007). Thermal conductivity in multi-wall carbon nanotube/silica-based nanocomposites. *Scripta Materialia*, 56(4), 265–268. <https://doi.org/10.1016/j.scriptamat.2006.10.025>
- Song, P. C., Liu, C. H., & Fan, S. S. (2006). Improving the thermal conductivity of nanocomposites by increasing the length efficiency of loading carbon nanotubes. *Applied Physics Letters*, 88(15), 153111. <https://doi.org/10.1063/1.2194267>
- Song, Y. S., & Youn, J. R. (2006). Evaluation of effective thermal conductivity for carbon nanotube/polymer composites using control volume finite element method. *Carbon*, 44(4), 710–717. <https://doi.org/10.1016/j.carbon.2005.09.034>
- Thostenson, E. T., Ren, Z., & Chou, T.-W. (2001). Advances in the science and technology of carbon nanotubes and their composites: a review. *Composites Science and Technology*, 61(13), 1899–1912. [https://doi.org/10.1016/S0266-3538\(01\)00094-X](https://doi.org/10.1016/S0266-3538(01)00094-X)
- Wang, F.-C., Zhang, Z.-H., Sun, Y.-J., Liu, Y., Hu, Z.-Y., Wang, H., Korznikov, A. V., Korznikova, E., Liu, Z.-F., & Osamu, S. (2015). Rapid and low temperature spark plasma sintering synthesis of novel carbon nanotube reinforced titanium matrix composites. *Carbon*, 95, 396–407.
- Wang, X., Jiang, Q., Xu, W., Cai, W., Inoue, Y., & Zhu, Y. (2013). Effect of carbon nanotube length on thermal, electrical and mechanical properties of CNT/bismaleimide composites. *Carbon*, 53, 145–152.
- Zheng, Y. F., Yao, X., Su, Y. J., & Zhang, D. L. (2016). Fabrication of an in-situ Ti-2.6vol%TiC metal matrix composite by thermomechanical consolidation of a TiH<sub>2</sub>-1vol%CNTs powder blend. *Materials Science and Engineering: A*, 667, 300–310. <https://doi.org/10.1016/j.msea.2016.04.096>
- Zhuang, J., Gu, D., Xi, L., Lin, K., Fang, Y., & Wang, R. (2020). Preparation method and underlying mechanism of MWCNTs/Ti6Al4V nanocomposite powder for selective laser melting additive manufacturing. *Powder Technology*, 368, 59–69. <https://doi.org/10.1016/j.powtec.2020.04.041>